Electromagnetics, 23:647–663, 2003

ISSN: 0272-6343 print/1532-527X online
DOI: 10.1080/02726340390244770

Taylor & Francis
Taylor & Francis Group

Effective Permittivity of Metallic Crystals: A Periodic Green's Function Formulation

MÁRIO G. SILVEIRINHA
CARLOS A. FERNANDES

Technical University of Lisbon
Instituto de Telecomunicações
Lisboa, Portugal

In this paper, we propose a periodic Green's function–based method for computing the static effective permittivity of metallic crystals. The method is valid for arbitrary lattice structures and inclusion shapes. We show that the homogenization problem can be reduced to an integral equation over the boundary of a generic metallic inclusion. The kernel of the integral equation is a periodic Green's function. This Green's function corresponds to the static potential from a three-dimensional array of point charges plus a uniform density of charge. Different representations of the Green's function are presented and discussed. We apply the developed formalism to characterize the effective permittivity of a three-dimensional array of thin metallic wires.

Keywords effective permittivity, artificial dielectric, artificial medium, metallic crystal, wire medium

Introduction

Artificial materials are composite structures formed by metallic(dielectric inclusions, periodically or randomly embedded in a host medium. As long as the wavelength of radiation is much larger than the characteristic dimension of the composite structure, the interaction of electromagnetic waves with artificial materials can be described by an averaged electromagnetic response, in analogy with the propagation of radiation in matter (Kranendonk & Sipes, 1977). Within this macroscopic average perspective, the artificial structure is characterized in the long wavelength limit by an effective permittivity and an effective permeability (Collin, 1991).

Our interest in artificial materials at the long wavelength regime is mainly related to their application to lens antennas, an idea thoroughly investigated in the sixties (Brown, 1969) that is becoming interesting again due to current advances in microfabrication techniques. The simpler-to-fabricate artificial media are in general anisotropic. Based on this fact, we recently proposed the synthesis of lens antennas with anisotropic artificial material substrate, explicitly taking into account the effect of anisotropy (Silveirinha & Fernandes, 2002).

This work was funded by "Fundação para a Ciência e Tecnologia" under project POSI 1999/CPS/34860.

Address correspondence to Mário G. Silveirinha, Departamento de Engenharia Electrotécnica, Polo II da Universidade de Coimbra, 3030 Coimbra, Portugal. E-mail: mario.silveirinha@co.it.pt

Computation of the effective parameters of artificial media is an old subject. The first systematic analysis of this problem seems to date back to the work of Lord Rayleigh (Rayleigh, 1892), who investigated the influence of spherical obstacles, arranged into a cubic lattice, on the properties of a medium. Rayleigh's formalism was later made numerically exact and generalized to other lattice structures (McPhedran & McKenzie, 1978; Doyle, 1978) and multiphase materials (Whites, 2000; Wu & Whites, 2001). It also inspired the KKR (Korringa-Kohn-Rostoker) band-structure procedure (Callaway, 1991), utilized for computing the dispersion characteristic of periodic structures. The effective permittivity can be obtained from the slope of the dispersion characteristic at the origin of the Brillouin zone (Lamb, Wood, & Ashcroft, 1980).

Although Rayleigh's formulation is numerically exact, it is restricted to media with spherical inclusions. The plane wave expansion method presented in Datta et al. (1993) allows characterizing dielectric crystals with arbitrary inclusion shapes. However, for high dielectric contrasts the method may suffer from convergence problems. An alternative method for computing the effective parameters of a composite material consists in matching the fields scattered from a truncated sample of material with those scattered from a homogeneous ideal material with the same canonical shape (Siqueira & Sarabandi, 2000).

The homogenization problem in periodic crystals can be reduced to a boundary value problem in a unit cell. In Karkkainen, Shivola, and Nikoskinen (2001) the boundary value problem is solved using a finite difference method and periodic boundary conditions. An alternative solution based on the boundary element method is presented in Sareni, Krahenbuhl, and Beroual (1996) and Sareni et al. (1997). The approach involves the discretization of the metallic–dielectric interfaces of the composite medium, as well as the boundary of the unit cell (to enforce the appropriate periodic boundary conditions).

In Wu and Whites (2001), a very interesting methodology is developed for computing the effective permittivity of simple cubic lattices of particles. It is still based on the boundary element method, but unlike the method proposed in Sareni, Krahenbuhl, and Beroual (1996), it does not require the discretization of the unit cell boundary. This is accomplished by incorporating the interaction between the inclusions directly into the kernel of the integral equation. However, the method fails to describe noncubic lattices, and the numerical evaluation of the integral equation kernel is inefficient.

In this paper, we propose a periodic Green's function formulation for calculating the effective permittivity of a metallic crystal. The method is general and is valid for arbitrary lattice structures and inclusion shapes. We reduce the homogenization problem to the solution of an integral equation over the boundary of a generic metallic inclusion. The kernel of the integral equation is the normalized electric potential from a three-dimensional array of point charges at the lattice points of the crystal and from a uniform density of charge, which guarantees the electric neutrality of the source distribution. We present and discuss different representations for the periodic electric potential, which allow the efficient computation of the integral equation kernel and thus of the effective permittivity.

We apply the developed formalism to calculate the static effective permittivity of a three-dimensional array of thin straight metallic wires, known as "wire medium" (Blanchard, Newman, & Peters, 1994; Peters & Newman, 1995; Moses & Engheta, 2001). We adopt the usual thin wire approximation for solving the pertinent integral equation. We derive an analytical formula for the periodic analog of the thin wire kernel used in the theory of linear antennas. Finally, we present numerical examples that illustrate the dependence of the effective permittivity of the wire medium on the parameters

that define its geometry. These results are useful for dimensioning the medium parameters in a practical application.

Previous studies on wire media are based on the computation of the dispersion characteristic. Blanchard, Newman, and Peters (1994) and Peters and Newman (1995) utilized the periodic moment method to set up a matrix equation for the currents in a unit cell. The dispersion characteristic is then calculated by setting the determinant of the impedance matrix to zero. Moses and Engheta (2001) used instead an approximate periodically loaded transmission line model. Each elementary plane of the artificial material is characterized using the periodic moment method. Single mode propagation is assumed in the interplane region, and the periodic structure theory is utilized to determine the dispersion characteristic of the overall medium.

Homogenization Problem in Metallic Crystals

We consider a periodic (three-dimensional) array of metallic inclusions embedded in air. The lattice primitive vectors are $\mathbf{a}_1$, $\mathbf{a}_2$, and $\mathbf{a}_3$. The periodic structure is invariant to translations along the primitive vectors. The primitive vectors may be rather arbitrary, apart from being independent. We denote the crystal unit cell by Ω and a generic observation point by $\mathbf{r} = (x_1, x_2, x_3)$. We take Ω as

$$\Omega = \{\alpha_1\mathbf{a}_1 + \alpha_2\mathbf{a}_2 + \alpha_3\mathbf{a}_3 : |\alpha_i| \leq 1/2\}. \tag{1}$$

The geometry of the unit cell is as depicted in Figure 1. We denote the metallic region in Ω by D. For simplicity, we assume that domain D is connected and does not intersect the unit cell's boundary $\partial\Omega$. The boundary of D is denoted by ∂D, and the corresponding unit normal vector oriented to the exterior of D, by $\hat{\mathbf{v}}$.

We investigate the relation between the local properties of the periodic structure and its macroscopic behavior. Our analysis considers that the radiation wavelength is much larger than the spacing between the inclusions. In these circumstances a purely static analysis is sufficient to characterize the effective medium parameters. Of course, for smaller wavelengths—sometimes still large when compared with the lattice constant—the metallic crystal cannot in general be described only in terms of permittivity–permeability

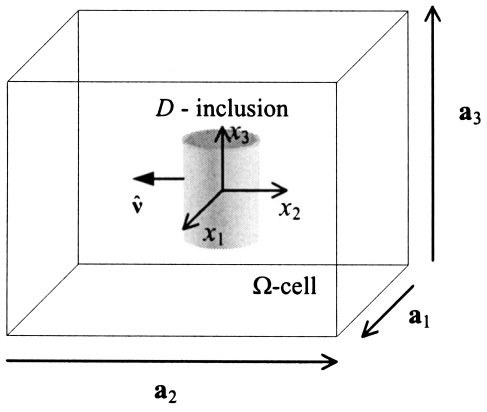

Figure 1. Geometry of the unit cell. The metallic region within the unit cell is D. The outward unit vector normal to the inclusion's boundary also is depicted.

dyadics, since chiral effects (Lindell et al., 1994), or in general bianisotropic effects, may emerge. Moreover, for wavelengths comparable to the lattice constant, the crystal has in general directional band-gaps (Sakoda, 2001). All these effects are out of the scope of the present analysis, which applies only for very large wavelengths. Ahead, we shall discuss with more detail the validity of the method.

Because we consider the static regime, the electric field $\mathbf{E}$ derives from an electric potential ϕ. The electric potential satisfies Laplace's equation and is constant over the metallic inclusions. We have thus:

$$\mathbf{E} = -\nabla\phi, \tag{2a}$$

$$\nabla^2\phi = 0, \qquad \phi = c_{\mathbf{I}} \text{ over } \partial D_{\mathbf{I}}, \tag{2b}$$

where $c_{\mathbf{I}}$ is a constant and $\partial D_{\mathbf{I}}$ is the boundary of the $\mathbf{I}$th metallic inclusion, which corresponds to the translation of D into the lattice point $\mathbf{r}_{\mathbf{I}} = i_1\mathbf{a}_1 + i_2\mathbf{a}_2 + i_3\mathbf{a}_3$ ($\mathbf{I} = i_1, i_2, i_3$) is a multi-index of integers).

We look for periodic solutions for the electric field $\mathbf{E}$. The corresponding electric potential is necessarily of the form

$$\phi = \phi^{\text{av}} + \phi^s, \qquad \phi^{\text{av}} = -\mathbf{E}_{\text{av}}.\mathbf{r}, \tag{2c}$$

where $\mathbf{E}_{\text{av}}$ is the average of the electric field over the unit cell and ϕ^s is a periodic potential. Potential ϕ^{av} is the electric potential from the (macroscopic) average field, while potential ϕ^s can be regarded as a scattered potential. As is well known (Shivola, 1999), the macroscopic average field differs from the "applied field" originated by the external sources.

Because the metallic crystal must be electrically neutral, the total charge in a connected inclusion must be zero. Therefore, we have the additional condition:

$$\int_{\partial D} \sigma_c ds = 0, \qquad \sigma_c = -\varepsilon_0 \partial\phi/\partial\mathbf{v}, \tag{2d}$$

where σ_c is the surface density of charge at inclusion D, ε_0 is free-space's permittivity, and $\partial/\partial\mathbf{v}$ stands for the normal derivative at ∂D.

The metallic crystal effective permittivity is calculated as follows. For a given (macroscopic) average electric field, the corresponding electric displacement $\mathbf{D}$ is

$$\mathbf{D} = \varepsilon_0\mathbf{E}_{\text{av}} + \frac{1}{\text{V}_{\text{cell}}}\mathbf{p}, \tag{3}$$

where $\text{V}_{\text{cell}} = |\mathbf{a}_1 \times \mathbf{a}_2.\mathbf{a}_3|$ is the volume of Ω, and $\mathbf{p}$ is the electric dipole moment of the metallic inclusion contained in Ω:

$$\mathbf{p} = \int_{\partial D} \mathbf{r}\sigma_c ds. \tag{4}$$

The (relative) effective permittivity dyadic is defined so that $\mathbf{D} = \varepsilon_0\overline{\overline{\varepsilon_{r,eff}}}\mathbf{E}_{\text{av}}$ for every macroscopic average field. Let $\mathbf{E}_{(n)} = -\nabla\phi_{(n)}$ be the electric field with average $\mathbf{E}_{\text{av},(n)} = E_{\text{av}}\hat{\mathbf{u}}_n$, where $\hat{\mathbf{u}}_n$ is a unit vector directed along the x_n-axis, $n = 1, 2, 3$. We have, thus,

$$\hat{\mathbf{u}}_m.\overline{\overline{\varepsilon_{r,eff}}}.\hat{\mathbf{u}}_n = \delta_{n,m} + \frac{\hat{\mathbf{u}}_m.\mathbf{p}_{(n)}}{\text{V}_{\text{cell}}\varepsilon_0 E_{\text{av}}}, \qquad n, m = 1, 2, 3, \tag{5}$$

where $\delta_{n,m}$ is the Kronecker δ-symbol and $\mathbf{p}_{(n)}$ is the electric dipole moment corresponding to field $\mathbf{E}_{(n)}$.

Integral Equation Formulation of the Homogenization Problem

We derive next an integral representation for the electric potential ϕ, in terms of the surface density of charge at the boundary of a generic metallic inclusion. To this end, we introduce the periodic Green's function $\Phi_{p0}(\mathbf{r}|\mathbf{r}')$, which satisfies

$$\nabla^2\Phi_{p0} = -\sum_{\mathbf{I}}\delta(\mathbf{r}-\mathbf{r}'-\mathbf{r}_\mathbf{I}) + \frac{1}{\mathrm{V_{cell}}}, \qquad \mathbf{r}_\mathbf{I} = i_1\mathbf{a}_1 + i_2\mathbf{a}_2 + i_3\mathbf{a}_3, \tag{6}$$

where $\mathbf{r}$ is the observation point, $\mathbf{r}'$ is a source point, $\mathbf{I} + (i_1, i_2, i_3)$ is a multi-index of integers, and δ is Dirac's δ-distribution. Green's function $\Phi_{p0}(\mathbf{r}|\mathbf{r}')$ is the normalized electric potential from an infinite array of point charges placed at $\mathbf{r}' + \mathbf{r}_\mathbf{I}$ and from the uniform density of charge corresponding to term $1/\mathrm{V_{cell}}$. The average charge in a unit cell, (i.e., the average of the right-hand side of (6)), is zero. This condition ensures that potential Φ_{p0} is periodic. As Φ_{p0} is an (normalized) electric potential, it is defined apart from the sum of an arbitrary constant. In the appendix we present several representations for Φ_{p0} and discuss their relative convergence rates.

To begin with, we note that from (2.b) and (2.c), the periodic potential ϕ^s verifies Laplace's equation. Thus, from (6) and from the Green's theorem we have that

$$\begin{aligned}&\nabla'.\{\Phi_{p0}(\mathbf{r}|\mathbf{r}')\nabla'\phi^s(\mathbf{r}') - \phi^s(\mathbf{r}')\nabla'\Phi_{p0}(\mathbf{r}|\mathbf{r}')\}\\ &\qquad = \phi^s(\mathbf{r}')\left(\sum_{\mathbf{I}}\delta(\mathbf{r}-\mathbf{r}'-\mathbf{r}_\mathbf{I}) - \frac{1}{\mathrm{V_{cell}}}\right),\end{aligned} \tag{7}$$

where the prime in symbol ∇' indicates that the gradient operates over the primed coordinates. Since ϕ^s is periodic we have that $\phi^s(\mathbf{r}-\mathbf{r}_\mathbf{I}) = \phi^2(\mathbf{r})$. Therefore, the above equation can be rewritten as

$$\begin{aligned}&\nabla'.\{\Phi_{p0}(\mathbf{r}|\mathbf{r}')\nabla'\phi^s(\mathbf{r}') - \phi^s(\mathbf{r}')\nabla'\Phi_{p0}(\mathbf{r}|\mathbf{r}')\}\\ &\qquad = \phi^s(\mathbf{r})\sum_{\mathbf{I}}\delta(\mathbf{r}-\mathbf{r}'-\mathbf{r}_\mathbf{I}) - \phi^s(\mathbf{r}')\frac{1}{\mathrm{V_{cell}}}.\end{aligned} \tag{8}$$

Next, we integrate both sides of the previous equation over the air region of the unit cell, i.e., $\Omega - D$. From the divergence theorem the integral corresponding to the left-hand-side term of (8) can be transformed into two surface integrals: one over the boundary of the unit cell and the other over the boundary of D. Since both Φ_{p0} and ϕ^s are periodic potentials, the surface integral over the boundary of the unit cell vanishes. We obtain, thus,

$$\phi^s(\mathbf{r}) = C + \int_{\partial D}\phi^s(\mathbf{r}')\frac{\partial\Phi_{p0}}{\partial\mathbf{v}'}(\mathbf{r}|\mathbf{r}') - \Phi_{p0}(\mathbf{r}|\mathbf{r}')\frac{\partial\phi^s}{\partial\mathbf{v}'}(\mathbf{r}')ds', \tag{9}$$

where the observation point $\mathbf{r}$ lies in the air region of the metallic crystal and C stands for a generic constant independent of the observation point.

On the other hand, since $\phi^{\text{av}} = -\mathbf{E}_{\text{av}}.\mathbf{r}$ verifies Laplace's equation, it satisfies an identity analogous to (7). Integrating the referred identity over the metallic region D, and transforming the divergence term into a surface integral over ∂D, we have that

$$0 = \int_{\partial D} \phi^{\text{av}}(\mathbf{r}') \frac{\partial \Phi_{p0}}{\partial \mathbf{v}'}(\mathbf{r}|\mathbf{r}') - \frac{\partial \phi^{\text{av}}}{\partial \mathbf{v}'} \Phi_{p0}(\mathbf{r}|\mathbf{r}') ds' + C. \tag{10}$$

In the previous formula, the observation point $\mathbf{r}$ lies in the air region of the metallic crystal, and C stands for a constant. Adding now equations (9) and (10) term by term, and using (2.d), we conclude that

$$\phi^s(\mathbf{r}) = C + \int_{\partial D} \phi(\mathbf{r}') \frac{\partial \Phi_{p0}}{\partial \mathbf{v}'}(\mathbf{r}|\mathbf{r}') + \frac{\sigma_c(\mathbf{r}')}{\varepsilon_0} \Phi_{p0}(\mathbf{r}|\mathbf{r}') ds', \qquad \mathbf{r} \text{ in the air region.} \tag{11}$$

However, since from (2.b) potential ϕ is constant over ∂D, it can be verified that

$$\int_{\partial D} \phi(\mathbf{r}') \frac{\partial \Phi_{p0}}{\partial \mathbf{v}'}(\mathbf{r}|\mathbf{r}') ds' = \phi|_{\partial D} \int_{\partial D} \frac{\partial \Phi_{p0}}{\partial \mathbf{v}'}(\mathbf{r}|\mathbf{r}') ds' = C, \qquad \mathbf{r} \text{ in the air region,} \tag{12}$$

where C stands for a generic constant, and the second identity is a consequence of (6) and of the divergence theorem. It follows thus that potential $\phi = \phi^{\text{av}} + \phi^s$ has the following integral representation:

$$\phi(\mathbf{r}) + \mathbf{E}_{\text{av}}.\mathbf{r} = C + \int_{\partial D} \frac{\sigma_c(\mathbf{r}')}{\varepsilon_0} \Phi_{p0}(\mathbf{r}|\mathbf{r}') ds', \qquad \mathbf{r} \text{ in the air region.} \tag{13}$$

From this integral representation we can obtain an integral equation for the unknown σ_c. Indeed, letting the observation point $\mathbf{r}$ approach the (connected) metallic surface ∂D and using (2.b), we find that

$$\mathbf{E}_{\text{av}}.\mathbf{r} = C + \int_{\partial D} \frac{\sigma_c(\mathbf{r}')}{\varepsilon_0} \Phi_{p0}(\mathbf{r}|\mathbf{r}') ds', \qquad \mathbf{r} \in \partial D, \tag{14}$$

where C stands for a constant. Thus, for a given macroscopic average field $\mathbf{E}_{\text{av}}$, we can determine the corresponding surface density of charge by solving the above integral equation subject to the electric neutrality condition (2.d) (which allows determining the value of constant C).

Straight Thin Wire Inclusions

Next we consider the particular case in which the inclusions are straight thin metallic wires, with radius a_w and length L_w. The corresponding metallic crystal commonly is named "Wire medium" (Moses & Engheta, 2001).

The plane defined by the primitive vectors $\mathbf{a}_1$ and $\mathbf{a}_2$ is referred to as the transversal plane. The direction normal to the transversal plane is by definition the $\perp$-direction. A generic vector $\mathbf{r}$ has the decomposition $\mathbf{r} = \mathbf{r}_{\parallel} + r_{\perp}\hat{\mathbf{u}}_{\perp}$, where $\hat{\mathbf{u}}_{\perp}$ is a unit vector directed along the $\perp$-direction, $r_{\perp}$ is the projection of $\mathbf{r}$ onto $\hat{\mathbf{u}}_{\perp}$, and $\mathbf{r}_{\parallel}$ is the projection of $\mathbf{r}$ onto the transversal plane.

We assume that the wire inclusions are parallel to the $\perp$-direction. Moreover, we consider that $a_w \ll L_w$, so that the thin wire condition holds. Thus, the density of charge σ_c induced at the surface of the inclusions is, to a first approximation, invariant to rotations around the wire axis.

To be more specific, let us consider the following parameterization for the wire contained in the unit cell:

$$\begin{gathered}\partial D = \mathbf{r}_w = a_w(\cos\varphi\hat{\mathbf{u}}_{T,1} + \sin\varphi\hat{\mathbf{u}}_{T,2}) + r_\perp\hat{\mathbf{u}}_\perp, \\ r_\perp \in [-L_w/2, L_w/2], \quad \varphi \in [0, 2\pi],\end{gathered} \tag{15}$$

where $\hat{\mathbf{u}}_{T,1}$ and $\hat{\mathbf{u}}_{T,2}$ form an orthonormal base of the transversal plane. Then, within the thin wire approximation, we have $\sigma_c(r_\perp, \varphi) \approx \sigma_c(r_\perp)$, and therefore integral equation (14) simplifies to

$$\mathbf{E}_{\text{av}}.\mathbf{r} + C \approx 2\pi a_w \int_{-L_w/2}^{L_w/2} \frac{\sigma_c(r'_\perp)}{\varepsilon_0}\left(\frac{1}{2\pi}\int_0^{2\pi} \Phi_{p0}(\mathbf{r}|\mathbf{r}'_w)d\varphi'\right)dr'_\perp, \qquad \mathbf{r} \in \partial D, \tag{16}$$

where $\mathbf{r}'_w = a_w(\cos\varphi'\hat{\mathbf{u}}_{T,1} + \sin\varphi'\hat{\mathbf{u}}_{T,2}) + r'_\perp\hat{\mathbf{u}}_\perp$. Strictly speaking, this integral equation does not have solution for $\mathbf{r} \in \partial D$, because we have reduced the degrees of freedom of the unknown. To avoid this situation we could, for example, restrict the observation point to the axis of the wire. We follow, however, a slightly different approach. We replace $\mathbf{r}$ in (16) by $\mathbf{r}_w$, and integrate both sides of the resulting equation in order to φ. In this way we obtain

$$\begin{gathered}r_\perp\mathbf{E}_{\text{av}}.\hat{\mathbf{u}}_\perp + C = 2\pi a_w \int_{-L_w/2}^{L_w/2} \frac{\sigma_c(r'_\perp)}{\varepsilon_0} K_{p0,w}(r_\perp|r'_\perp)dr'_\perp, \\ r_\perp \in [-L_w/2, L_w/2],\end{gathered} \tag{17}$$

where we have defined $K_{p0,w}(r_\perp|r'_\perp)$ as the static periodic thin wire kernel, given by

$$K_{p0,w}(r_\perp|r'_\perp) = \frac{1}{(2\pi)^2}\int_0^{2\pi}\int_0^{2\pi} \Phi_{p0}(\mathbf{r}_w|\mathbf{r}'_w)d\varphi' d\varphi. \tag{18}$$

This kernel can be calculated in closed analytical form using the spectral-like representation of the periodic Green's function derived in the appendix. In fact, from (32.a) we readily obtain

$$K_{p0,w}(r_\perp|r'_\perp) = \sum_{\bar{\mathbf{J}}} A_{\Phi 0,\bar{\mathbf{J}}}(u_\perp)[J_0(a_w|\mathbf{k}^0_{\bar{\mathbf{J}},\parallel}|)]^2, \qquad u_\perp = r_\perp - r'_\perp, \tag{19}$$

where J_0 is the Bessel function of first kind and order 0, and the rest of the symbols are defined as in the appendix. Formula (19) is valid provided $|u_\perp| < |a_{3\perp}|$, where $a_{3\perp} = \mathbf{a}_3.\hat{\mathbf{u}}_\perp$. However, as Φ_{p0} is invariant to translations along the primitive vector $\mathbf{a}_3$, we can prove that in general we have

$$\begin{gathered}K_{p0,w}(r_\perp + la_{3\perp}|r'_\perp) = \sum_{\bar{\mathbf{J}}} A_{\Phi 0,\bar{\mathbf{J}}}(u_\perp)e^{jl\mathbf{k}^0_{\bar{\mathbf{J}},\parallel}.\mathbf{a}_3}[J_0(a_w|\mathbf{k}^0_{\bar{\mathbf{J}},\parallel}|)]^2, \\ l \text{ arbitrary integer},\end{gathered} \tag{20}$$

where, as before, $|u_\perp| < |a_{3\perp}|$. In the particular case of $\mathbf{a}_3$ being orthogonal to the transversal plane, function $K_{p0,w}$ is periodic.

Kernel $K_{p0,w}$ has a logarithmic singularity at points of the form $u_\perp = la_{3\perp}$, where l is an arbitrary integer. This result follows from the fact that the free space's thin wire kernel used in the theory of linear antennas has the same singular behavior at the source point (Pearson, 1975). The spectral-like representation (19) converges slowly close to the singular points. The convergence problems can be avoided by computing $K_{p0,w}$ directly from (18), using the mixed-domain representation derived in the appendix.

Integral equation (17) is solved numerically using the method of moments (MoM). The unknown density $\sigma_c(r_\perp)$ has a boundary edge singularity at the ends of the wire. It grows to infinity as $1/\sqrt{d}$, where d is the distance to the end of the wire. We thus assume in the numerical implementation that $\sigma_c(r_\perp)$ is of the form $\sigma_c(r_\perp) = f(r_\perp)/\sqrt{(L_w/2)^2 - r_\perp^2}$, where $f_(r_\perp)$ is a well-behaved function. Function $f(r_\perp)$ is expanded in subdomain triangular functions. The details of the discretization of the integral equation are standard, and thus are omitted.

Numerical Examples

In this section we present numerical examples that illustrate the application of the developed formalism and characterize the effective permittivity of the wire medium.

The direct lattice primitive vectors are assumed to be of the form $\mathbf{a}_1 = (a_\parallel, 0, 0)$, $\mathbf{a}_2 = (0, a_\parallel, 0)$, and $\mathbf{a}_3 = (0, 0, a_\perp)$. The wire axes are normal to the plane formed by $\mathbf{a}_1$ and $\mathbf{a}_2$.

From (17) it is clear that within thin wire approximation, the effective permittivity dyadic is of the form

$$\overline{\overline{\varepsilon_{r,eff}}} = (\hat{\mathbf{u}}_1\hat{\mathbf{u}}_1 + \hat{\mathbf{u}}_2\hat{\mathbf{u}}_2) + \varepsilon_{r\perp}\hat{\mathbf{u}}_\perp\hat{\mathbf{u}}_\perp. \tag{21}$$

Therefore, the wire medium is uniaxial anisotropic. Since the volume fraction of the wire inclusions is in general very small, the magnetic effects can be neglected in the long wavelength limit.

The numerical results are computed using 16 subdomain expansion functions in the MoM implementation. The computation time for a specific geometry is about 1 minute in a Pentium-III 800MHz.

The previous analyses of the wire medium are mainly focused on the study of its dynamic properties (Blanchard, Newman, & Peters, 1994; Moses & Engheta, 2001). Nevertheless, we have compared successfully the long wavelength results of the referred papers with our method. For example, our method yields that the relative effective permittivity of a crystal with $a_w/a_\parallel = 0.1$, $L_w/a_\perp = 0.86$, and $a_\perp/a_\parallel = 7$ is $\varepsilon_{r\perp} = 4.2$, in good agreement with the asymptotic behavior of the results of (Blanchard, Newman, & Peters, 1994), as the number of expansion functions in their MoM implementation increases.

In the first example we consider that $a_\parallel$ is kept fixed. The normalized wire radius is $a_w/a_\parallel = 0.1$, and $a_\perp/a_\parallel$ is 1, 5, or 7. The corresponding effective permittivity in the $\perp$-direction (parallel to the wires) is depicted in Figure 2 as function of the normalized wire length. As expected, $\varepsilon_{r\perp}$ increases with the wire length and $a_\perp/a_\parallel$. It is apparent from the figure that by choosing the wire medium parameters adequately, it is possible to synthesize an artificial medium with a desired anisotropy ratio.

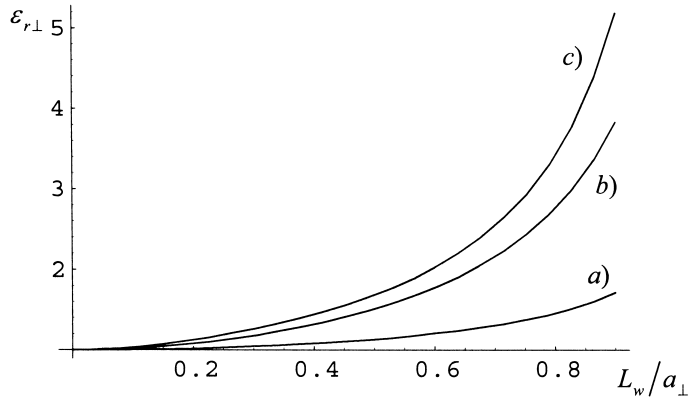

Figure 2. $\perp$-direction relative permittivity in function of the normalized wire length: (a) $a_\perp/a_\parallel = 1$, (b) $a_\perp/a_\parallel = 4$, (c) $a_\perp/a_\parallel = 7$. The normalized wire radius is $a_w/a_\parallel = 0.1$.

As the normalized wire length $L_w/a_\perp$ approaches unity, the ends of adjacent wires are progressively closer, and thus permittivity $\varepsilon_{r\perp}$ approaches infinity. In the limit situation of a crystal with infinitely long wires, the extraordinary wave degenerates into a transverse electromagnetic wave (relative to the wire axes), which sees an infinite permittivity along the $\perp$-direction.

In Figure 3 we present the variation of $\varepsilon_{r\perp}$ with the normalized wire radius, for $a_\perp/a_\parallel = 7$ and $L_w/a_\perp = 0.8$. It is remarkable that, even for very thin wires and thus for extremely low inclusion volume fractions, the anisotropy ratio remains relatively high.

In Figure 4 we depict $\varepsilon_{r\perp}$ as a function of the wire distance in the $\perp$-direction. The wire length and the wire radius are kept fixed, equal to $L_w/a_\parallel = 0.8$ and $a_w/a_\parallel = 0.1$, respectively. As expected, permittivity $\varepsilon_{r\perp}$ increases as the wire distance decreases.

To conclude, we investigate the scope of application of the presented results. This requires studying the dependence of the effective permittivity with frequency. To this end, we have computed the band structure of the wire medium using the 3D analog of the hybrid method proposed in Silveirinha and Fernandes (in press). Then, from the slope of

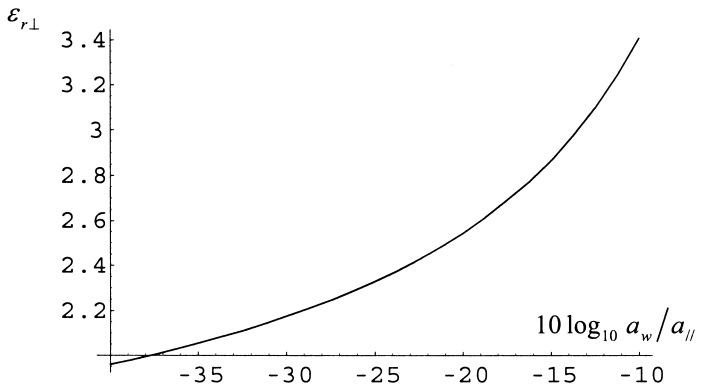

Figure 3. $\perp$-direction relative permittivity in function of the normalized wire radius. In this example $a_\perp/a_\parallel = 7$ and $L_w/a_\perp = 0.8$.

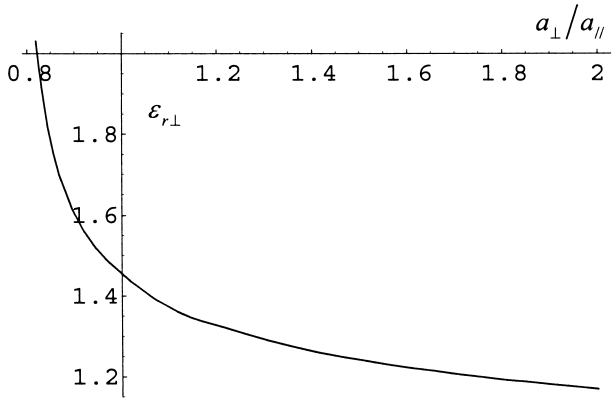

Figure 4. $\perp$-direction relative permittivity in function of $a_\perp/a_\parallel$. In this example $a_w/a_\parallel = 0.1$ and $L_w/a_\parallel = 0.8$.

the appropriate fundamental band we have extracted $\varepsilon_{r\perp}$ as a function of the radiation wavelength λ.

The result for a crystal with $L_w/a_\perp = 0.86$, $a_\perp/a_\parallel = 7$, and $a_w/a_\parallel = 0.1$ is depicted in Figure 5. The method presented in this paper yields the value 4.2 for the effective permittivity of the metallic crystal. That value agrees exactly with that extracted from the slope of the dispersion curve. From Figure 5 it is apparent that for $\lambda/a_\perp > 10$ the effective permittivity is approximately constant, in accordance with a well-known rule of thumb. For smaller wavelengths the effective permittivity increases very fast. The crystal has a band gap (for propagation in the transversal plane), beginning at $\lambda/a_\perp = 1.8$.

Assuming that $a_\perp \geq a_\parallel$, the frequency region where the results of this paper apply is approximately defined by $\lambda/a_\perp > 2\sqrt{\varepsilon_{r\perp}}$. This rule is based on elementary results from photonic band gap theory, as discussed next. Indeed, nearby the origin of the Brillouin zone, the dispersion characteristic for propagation in the transversal plane is to a first approximation $\beta = k/\sqrt{\varepsilon_{r\perp}}$, where $\beta = 2\pi/\lambda$ is the free-space wave number and k is the amplitude of the wave vector. The largest sphere that fits in the Brillouin zone has

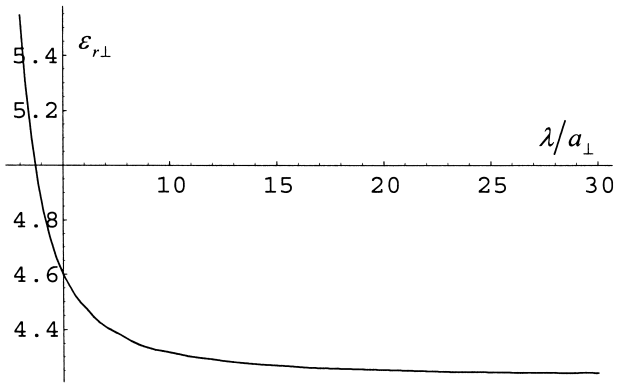

Figure 5. $\perp$-direction relative permittivity in function of the normalized free-space wavelength. In this example $a_w/a_\parallel = 0.1$, $L_w/a_\perp = 0.86$, and $a_\perp/a_\parallel = 7$.

radius $k = \pi/a_\perp$, which corresponds approximately to the wave number $\pi/(a_\perp\sqrt{\varepsilon_{r\perp}})$. It is thus reasonable to expect that for $\beta > \pi/(a_\perp\sqrt{\varepsilon_{r\perp}})$ the wire medium may not be described in terms of a permittivity dyadic (at least without considering either spatial or frequency dispersion). We find thus that our static results apply in case of $\lambda/a_\perp > 2\sqrt{\varepsilon_{r\perp}}$. In particular, we conclude that the bandwidth of the wire medium decreases as its permittivity increases.

Conclusions

We presented a new efficient method for the computation of the effective permittivity of metallic crystals. The method is valid for arbitrary lattice structures and inclusion shapes. The homogenization problem was reduced to an integral equation over the boundary of a generic inclusion. Several representations for the kernel of the integral equation, a triple-periodic Green's function, were derived. Of particular relevance is the mixed-representation, which has Gaussian convergence irrespective of the observation point position within the unit cell. This property is fundamental for the efficient computation of the effective permittivity of metallic crystals. The derived results were particularized to the wire medium case. Numerical examples that illustrate the dependence of the effective permittivity of the wire medium on the wire spacing, wire radius, and wire length were presented. A simple rule, concerning the validity of the proposed method, was derived.

Although in this paper we assumed the inclusions to be metallic, the proposed method can be easily generalized to dielectric crystals and also to the magnetic permeability homogenization problem (Silveirinha & Fernandes, 2002).

Appendix

In this appendix we derive different representations for the solution of equation (6), the periodic Green's function, and discuss their relative convergence rates. To begin with, we introduce an auxiliary Green's function, $\Phi_p(\mathbf{r};\mathbf{k})$, that satisfies

$$\nabla^2\Phi_p = -e^{-j\mathbf{k}.\mathbf{r}}\sum_{\mathbf{I}}\delta(\mathbf{r}-\mathbf{r}_\mathbf{I}), \qquad \mathbf{r}_\mathbf{I} = i_1\mathbf{a}_1 + i_2\mathbf{a}_2 + i_3\mathbf{a}_3, \tag{22}$$

where $\mathbf{k} = (k_1, k_2, k_3)$ is a wave vector and $\mathbf{I} = (i_1, i_2, i_3)$ is an arbitrary multi-index of integers. It can be verified by direct manipulations that Φ_{p0}, defined as follows, is a solution of (6):

$$\Phi_{p0}(\mathbf{r}|\mathbf{r}') = \lim_{\mathbf{k}\to 0}\left(\Phi_p(\mathbf{u};\mathbf{k}) - \frac{1}{\mathrm{V}_{\mathrm{cell}}}\frac{e^{-j\mathbf{k}.\mathbf{u}}}{|\mathbf{k}|^2}\right), \qquad \mathbf{u} = \mathbf{r}-\mathbf{r}'. \tag{23}$$

In the following sections, we derive different representations for Φ_p, and then, using the above formula, for Φ_{p0}.

Spectral Representation for the Periodic Green's Function

Since the auxiliary Green's function $\Phi_p(\mathbf{r};\mathbf{k})$ is a Floquet wave with wave vector $\mathbf{k}$, it can be expanded into plane waves. A generic plane wave has wave vector $\mathbf{k}_\mathbf{J} = \mathbf{k} + j_1\mathbf{b}_1 + j_2\mathbf{b}_2 + j_3\mathbf{b}_3$, where $\mathbf{J} = (j_1, j_2, j_3)$ is an arbitrary multi-index of integers, and $\mathbf{b}_1$, $\mathbf{b}_2$, and $\mathbf{b}_3$ are the reciprocal lattice primitive vectors defined by Callaway (1991):

$$\mathbf{a}_n.\mathbf{b}_m = 2\pi\delta_{n,m}, \qquad n, m = 1, 2, 3. \tag{24}$$

Straightforward calculations show that the spectral representation of Φ_p is

$$\Phi_p(\mathbf{r};\mathbf{k}) = \frac{1}{\mathrm{V_{cell}}}\sum_{\mathbf{J}} \frac{e^{-j\mathbf{k_J}.\mathbf{r}}}{|\mathbf{k_J}|^2}, \tag{25}$$

where $\mathrm{V_{cell}}$ is the volume of the unit cell. From (23) we obtain thus the spectral representation of Φ_{p0}:

$$\Phi_{p0}(\mathbf{r}|\mathbf{r}') = \frac{1}{\mathrm{V_{cell}}}\sum_{\mathbf{J}\neq 0} \frac{e^{-j\mathbf{k}^0_{\mathbf{J}}.\mathbf{u}}}{|\mathbf{k}^0_{\mathbf{J}}|^2}, \qquad \mathbf{k}^0_{\mathbf{J}} = j_1\mathbf{b}_1 + j_2\mathbf{b}_2 + j_3\mathbf{b}_3. \tag{26}$$

The spectral representation converges very slowly, and so it is useless for the numerical evaluation of the Green's function.

Since potential Φ_{p0} is static, it is defined apart from the sum of an arbitrary constant. Using, however, (23) to define Φ_{p0} the arbitrariness on the definition disappears. Indeed, Φ_{p0} defined as in (23) is the unique solution of (6) that satisfies

$$\int_\Omega \Phi_{p0}(\mathbf{u})d^3\mathbf{u} = 0. \tag{27}$$

Spectral-Like Representation

Next we derive an alternative representation for Φ_{p0} with improved convergence rate. As before, we compute first the auxiliary Green's function Φ_p. This Green's function corresponds to the static potential from a three-dimensional phase-shifted array of point sources. The phase-shift between adjacent elements of the array is defined by the wave vector $\mathbf{k}$. The idea is that we can regard the three-dimensional array of point sources as the superimposition of double-periodic arrays of point sources. To be more specific, let Φ_H be the solution of

$$\nabla^2\Phi_H = -e^{-j\mathbf{k}.\mathbf{r}}\sum_{\bar{\mathbf{I}}}\delta(\mathbf{r}-\mathbf{r}_{\bar{\mathbf{I}}}), \tag{28}$$

where $\mathbf{r}$ is an observation point, $\mathbf{r}_{\bar{\mathbf{I}}} = i_1\mathbf{a}_1 + i_2\mathbf{a}_2$ is a (transversal) lattice point, $\bar{\mathbf{I}} = (i_1, i_2)$ is a generic multi-index of integers, and $\mathbf{k}$ is the wave vector that defines the phase shift between the point sources. Function Φ_H corresponds to the static version of the usual "periodic Green's function" employed for characterizing double-periodic systems in a three-dimensional space (e.g., frequency selective surfaces, etc.). From (22) it is clear that

$$\Phi_p(\mathbf{r};\mathbf{k}) = \sum_n \Phi_H(\mathbf{r}-n\mathbf{a}_3;\mathbf{k})e^{-jn\mathbf{k}.\mathbf{a}_3}, \tag{29}$$

where n is an arbitrary integer. Function Φ_p is thus the superimposition of potentials from double-periodic arrays of point sources.

For convenience, we define the transversal plane as the plane defined by primitive vectors $\mathbf{a}_1$ and $\mathbf{a}_2$. The unit vector normal to the transversal plane is by definition

$\hat{\mathbf{u}}_\perp$. As is well known, Green's function Φ_H has the following spectral representation (e.g., Jorgenson & Mittra, 1990):

$$\Phi_H(\mathbf{r};\mathbf{k}) = \frac{1}{\mathrm{A_{cell}}} \sum_{\bar{\mathbf{J}}} \frac{e^{-|\mathbf{k}_{\bar{\mathbf{J}},\parallel}||r_\perp|}}{2|\mathbf{k}_{\bar{\mathbf{J}},\parallel}|} e^{-j\mathbf{k}_{\bar{\mathbf{J}},\parallel}.\mathbf{r}}, \qquad \mathrm{A_{cell}} = |\mathbf{a}_1 \times \mathbf{a}_2|, \tag{30}$$

where $\mathbf{k}_{\bar{\mathbf{J}},\parallel} = \mathbf{k}_\parallel + j_1\mathbf{b}_{1\parallel} + j_2\mathbf{b}_{2\parallel}$, $\bar{\mathbf{J}} = (j_1, j_2)$ is a multi-index of arbitrary integers, $\mathbf{k}_\parallel$ is the projection of $\mathbf{k}$ onto the transversal plane, $r_\perp$ is the projection of $\mathbf{r}$ onto $\hat{\mathbf{u}}_\perp$, and $\mathbf{b}_{1\parallel}$ and $\mathbf{b}_{2\parallel}$ are reciprocal lattice vectors that satisfy $\mathbf{a}_n.\mathbf{b}_{m\parallel} = 2\pi\delta_{n,m}$ for $n, m = 1, 2$, and lie on the transversal plane. It can be verified that $\mathbf{b}_{1\parallel}$ and $\mathbf{b}_{2\parallel}$ are equal to the projections of vectors $\mathbf{b}_1$ and $\mathbf{b}_2$, defined as in (24), onto the transversal plane.

The interesting point is that when we insert (30) into (29), the sum with index n can be calculated in closed analytical form, since it corresponds to two geometrical series (Silveirinha & Fernandes, in press). Indeed, provided $|r_\perp| < |a_{3\perp}|$ where $a_{3\perp} = \mathbf{a}_3.\hat{\mathbf{u}}_\perp$, we have that

$$\Phi_p(\mathbf{r};\mathbf{k}) = \frac{1}{\mathrm{A_{cell}}} \sum_{\bar{\mathbf{J}}} \frac{e^{-j\mathbf{k}_{\bar{\mathbf{J}},\parallel}.\mathbf{r}}}{2|\mathbf{k}_{\bar{\mathbf{J}},\parallel}|} \left(e^{-|k_{\bar{\mathbf{J}},\parallel}||r_\perp|} + \sum_{\pm} \frac{e^{\pm|\mathbf{k}_{\bar{\mathbf{J}},\parallel}|r_\perp}}{e^{|a_{3\perp}|(|\mathbf{k}_{\bar{\mathbf{J}},\parallel}| \pm jk_{\bar{\mathbf{J}},\perp})} - 1} \right), \tag{31}$$

where $\mathbf{k}_{\bar{\mathbf{J}}} = \mathbf{k} + j_1\mathbf{b}_1 + j_2\mathbf{b}_2$, $\mathbf{k}_{\bar{\mathbf{J}},\parallel}$, is the projection of $\mathbf{k}_{\bar{\mathbf{J}}}$ onto the transversal plane, and $k_{\bar{\mathbf{J}},\perp}$ is the projection of $\mathbf{k}_{\bar{\mathbf{J}}}$ onto $\hat{\mathbf{u}}_\perp$. In the above formula the sum with index "$\pm$" is a shorthand notation for the sum of two terms: one with the "$+$" sign and the other with the "$-$" sign. We refer to formula (31) as the spectral-like representation of Φ_p relative to the transversal plane defined by $\mathbf{a}_1$ and $\mathbf{a}_2$. This representation is valid for $|r_\perp| < |a_{3\perp}|$. However, since Φ_p is a Floquet potential with wave vector $\mathbf{k}$, it is always possible (by translations along primitive vector $\mathbf{a}_3$) to transform a point that does not satisfy $|r_\perp| < |a_{3\perp}|$ into an equivalent point where formula (31) can be applied. Thus, we can assume without loss of generality that $|r_\perp| < |a_{3\perp}|/2$. In this interval the spectral-like representation converges exponentially, except in the case $|r_\perp| = 0$, where the convergence is rather slow. Indeed, it is easy to verify that the convergence properties of Φ_p mimic those of Φ_H.

It is important to note that the roles of the direct lattice vectors $\mathbf{a}_1$, $\mathbf{a}_2$, and $\mathbf{a}_3$ can be interchanged by considering cyclic permutations of these vectors. In fact, we can consider three distinct transversal lattices. Therefore, we have at our disposal a total of three alternative spectral-like representations for Φ_p. One of these representations is precisely (31). The other two representations are analogous to (31), but with one important difference: as the transversal plane depends on the specific representation, so does the respective convergence rate. In fact, for each of these representations the region of slow convergence is the transversal lattice. Using this property it is easy to verify that it is always possible to choose a spectral-like representation such that $|r_\perp| \neq 0$, and thus such that the convergence is exponential. The only exception to this rule is the case $\mathbf{r} = \mathbf{0}$, which requires the use of acceleration techniques analogous to those employed for the computation of Φ_H (e.g., Jorgenson & Mittra, 1990), or alternatively the use of a different representation of the Green's function (see the next section).

From (23) and (31) we can now obtain the corresponding spectral-like representation for Φ_{p0}:

$$\Phi_{p0}(\mathbf{u}) = \sum_{\bar{\mathbf{J}}} A_{\Phi 0,\bar{\mathbf{J}}}(u_\perp) e^{-j\mathbf{k}^0_{\bar{\mathbf{J}},\parallel}\cdot\mathbf{u}}, \tag{32a}$$

$$A_{\Phi 0,\bar{\mathbf{J}}}(u_\perp) = \begin{cases} \dfrac{1}{2\mathrm{A}_{\mathrm{cell}}}\left(-|u_\perp| + \dfrac{u_\perp^2}{|a_{3\perp}|} + \dfrac{|a_{3\perp}|}{6}\right) & \text{if } \mathbf{J} = \mathbf{0}, \\ \dfrac{1}{\mathrm{A}_{\mathrm{cell}} 2|\mathbf{k}^0_{\bar{\mathbf{J}},\parallel}|}\left(e^{-|k^0_{\bar{\mathbf{J}},\parallel}||u_\perp|} + \displaystyle\sum_{\pm} \frac{e^{\pm|\mathbf{k}^0_{\bar{\mathbf{J}},\parallel}|u_\perp}}{e^{|a_{3\perp}|(|\mathbf{k}^0_{\bar{\mathbf{J}},\parallel}|\pm jk^0_{\bar{\mathbf{J}},\perp})} - 1}\right) & \text{if } \mathbf{J} \neq \mathbf{0}, \end{cases} \tag{32b}$$

where $\mathbf{k}^0_{\bar{\mathbf{J}}} = j_1\mathbf{b}_1 + j_2\mathbf{b}_2$. The convergence rate of the above formula is analogous to that of the case discussed previously. As before there exist three distinct spectral-like representations for Φ_{p0}, each with a different region of slow convergence.

Mixed Representation

We present next a mixed-domain representation for Φ_{p0}. This representation is derived using Ewald's error function representation of Φ_p (Ewald, 1921), together with formula (23). The result is:

$$\begin{aligned} \Phi_{p0} = \frac{1}{\mathrm{V}_{\mathrm{cell}}} \sum_{\mathbf{J}\neq\mathbf{0}} \left(\frac{1}{|\mathbf{k}^0_{\mathbf{J}}|^2} e^{-|\mathbf{k}^0_{\mathbf{J}}|^2/4E^2} e^{-j\mathbf{u}.\mathbf{k}^0_{\mathbf{J}}}\right) \\ - \frac{1}{\mathrm{V}_{\mathrm{cell}}}\frac{1}{4E^2} + \sum_{\mathbf{I}} \frac{1}{4\pi\rho_{\mathbf{I}}}(1 - \mathrm{erf}\, E\rho_{\mathbf{I}})), \end{aligned} \tag{33}$$

where $\mathbf{u} = \mathbf{r} - \mathbf{r}'$, $\rho_{\mathbf{I}} = |\mathbf{u} - \mathbf{r}_{\mathbf{I}}|$, and $\mathbf{k}^0_{\mathbf{J}} = j_1\mathbf{b}_1 + j_2\mathbf{b}_2 + j_3\mathbf{b}_3$. Symbols $\mathbf{I}$ and $\mathbf{J}$ denote a generic triple-index, and "erf" the error function. Parameter E is an arbitrary positive constant that defines the relative convergence rate of the spatial-like parcel (the sum with index $\mathbf{I}$) and the spectral-like parcel (the sum with index $\mathbf{J}$). A good choice for parameter E, which ensures similar convergence rates for the spatial-like and spectral-like sums, is $E = \sqrt{\pi}/\mathrm{V}_{\mathrm{cell}}^{1/3}$. The mixed-domain representation has, irrespective of the observation point, Gaussian convergence. Therefore, it has an excellent convergence rate.

Spatial Representation for the Periodic Green's Function

To conclude this appendix, and for the sake of completeness, we present a spatial representation for the periodic Green's function.

From elementary electrostatics (Jackson, 1999), the solution of (6) can be written as follows:

$$\Phi_{p0} = \int \left(\sum_{\mathbf{I}} \delta(\mathbf{u}' - \mathbf{r}_{\mathbf{I}}) - \frac{1}{\mathrm{V}_{\mathrm{cell}}}\right) \Phi_0(\mathbf{u} - \mathbf{u}') d^3\mathbf{u}', \qquad \mathbf{u} = \mathbf{r} - \mathbf{r}', \tag{34}$$

where $\Phi_0(\mathbf{r}) = 1/(4\pi r)$. The integration range in (34) is all space. The term inside the brackets corresponds to the total density of the electric charge (in normalized units).

In order to evaluate (34) we have to proceed with some care. Indeed, we cannot break (34) as a sum of two integrals, because, as the integration range is all space, they would diverge.

We thus make the following preliminary definitions. Let V be a bounded volume of space such that $V = -V$, i.e., that V is invariant to an inversion (or alternatively if $\mathbf{r}$ is in V then $-\mathbf{r}$ also is). For example, V can be sphere or a parallelepiped centered at the origin of space. We define the set $n.V$ as the set that contains the points of the form $n\mathbf{r}$, where $\mathbf{r}$ is a generic point of V and n is greater than 1. Geometrically $n.V$ is an expansion of the original set V. Obviously, if we let n go to infinity then $n.V$ becomes all space. Therefore we can rewrite (34) as

$$\Phi_{p0} = \lim_{n\to\infty} \int_{n.V} \left(\sum_{\mathbf{I}} \delta(\mathbf{u}' - \mathbf{r}_{\mathbf{I}}) - \frac{1}{\mathrm{V_{cell}}} \right) \Phi_0(\mathbf{u} - \mathbf{u}') d^3\mathbf{u}'. \tag{35}$$

The last equation is also equivalent to

$$\Phi_{p0} = \lim_{n\to\infty} \sum_{\mathbf{r}_{\mathbf{I}} \in n.V} \Phi_0(\mathbf{u} - \mathbf{r}_{\mathbf{I}}) - \frac{1}{\mathrm{V_{cell}}} \int_{n.V} \Phi_0(\mathbf{u} - \mathbf{u}') d^3\mathbf{u}'. \tag{36}$$

The first term in the right-hand side of equation (36) is the static potential from the point charges inside volume $n.V$, while the second term is the static potential from the uniform density of charge inside the same volume. In order to evaluate this second term we note that from the divergence theorem we have

$$\int_{n.V} \Phi_0(\mathbf{u} - \mathbf{u}') d^3\mathbf{u}' = \frac{1}{2} \int_{n.S} (\mathbf{u}' - \mathbf{u}).\hat{\mathbf{v}}' \Phi_0(\mathbf{u}' - \mathbf{u}) ds', \tag{37}$$

where surface S is the boundary of volume V, and $\hat{\mathbf{v}}$ is the outward unit vector normal to S. The right-hand side of the above equation is a surface integral over $n.S$. After straightforward calculations it can be verified that

$$\int_{n.V} \Phi_0(\mathbf{u} - \mathbf{u}') d^3\mathbf{u}' = n^2 C_{\Phi 0,V} - \frac{1}{2} \mathbf{u}.\overline{\overline{L}}.\mathbf{u} + O(1/n), \tag{38a}$$

$$C_{\Phi 0,V} = \frac{1}{8\pi} \int_S \hat{\mathbf{u}}'.\hat{\mathbf{v}}' ds', \tag{38b}$$

$$\overline{\overline{\mathbf{L}}} = \frac{1}{4\pi} \int_S \frac{\hat{\mathbf{v}}'\hat{\mathbf{u}}'}{|\mathbf{u}'|^2} ds', \tag{38c}$$

where $C_{\Phi 0,V}$ is a constant, $\overline{\overline{\mathbf{L}}}$ is a dyadic, and $O(1/n)$ is a term that converges to zero as n approaches infinity. It is important to note that constant $C_{\Phi 0,V}$ as well as dyadic $\overline{\overline{\mathbf{L}}}$ are independent of n and are completely determined by V. Moreover, dyadic $\overline{\overline{\mathbf{L}}}$ only depends on the geometrical shape of V and not on its specific volume. Very interestingly $\overline{\overline{\mathbf{L}}}$ is the so-called depolarization dyadic, utilized for determining the local field in homogenization theory (Shivola, 1999, p. 55). The depolarization dyadic is calculated in Yaghjian (1980) for several volume shapes.

From the previous results we conclude thus that the periodic Green's function has the following spatial representation:

$$\Phi_{p0}(\mathbf{r}|\mathbf{r}') = \lim_{n\to\infty}\left(\sum_{\mathbf{r_I}\in n.V}\Phi_0(\mathbf{u}-\mathbf{r_I}) - \frac{C_{\Phi 0,V}}{\mathrm{V_{cell}}}n^2\right) + \frac{1}{\mathrm{V_{cell}}}\frac{1}{2}\mathbf{u}.\overline{\overline{\mathbf{L}}}.\mathbf{u}. \qquad (39)$$

The first term of the spatial representation corresponds to a regularized sum of the point potentials, while the second term is a quadratic form. It is important to note that volume V defines the summation order of the point potentials. In fact, the series must be summed exactly as suggested by the limit form of equation (39), because it is not absolutely convergent. We also stress that the quadratic form only depends on the geometrical shape of the summation volume and that for different geometrical shapes we obtain, in general, different quadratic formulas. The convergence rate of formula (39) is poor. The periodic Green's function, defined as in (39), is not in general coincident with definition (23). The two representations differ from a constant.

An alternative proof of the derived results, for the case of the lattice primitive vectors being orthogonal, can be found in Silveirinha and Fernandes (2001).

References

Blanchard, J. L., E. H. Newman, and M. Peters. 1994. Integral equation analysis of artificial media. *IEEE Trans. on AP* 42:727.

Brown, J. 1969. Lens antennas. In *Antenna theory*, part 2, eds. R. E. Collin and F. J. Zucker, Inter-University Electronic Series, Vol. 7, pp. 104–150. New York: McGraw-Hill.

Callaway, J. 1991. *Quantum theory of solid state*, Chapter 1. New York: Academic Press.

Collin, R. E. 1991. *Field theory of guided waves*, 2nd ed., Chapter 12. New York: IEEE Press.

Datta, S., C. T. Chan, K. M. Ho, and C. M. Soukoulis. 1993. Effective dielectric constant of periodic composite structures. *Phys. Rev. B* 48:14936.

Doyle, W. T. 1978. The Clausius-Mossotti problem for cubic arrays of spheres. *J. Appl. Phys*. 49:795–797.

Ewald, P. P. 1921. Die Berechnung optischer und elektrostatischer Gitterpotentiale. *Ann. Der Physik* 64:253–287.

Jackson, H. D. 1999. *Classical electrodynamics*, 3rd ed. New York: John Wiley.

Jorgenson, R., and R. Mittra. 1990. Efficient calculation of the free-space periodic Green's function. *IEEE Trans. on AP* 38:633–642.

Karkkainen, K., A. Shivola, and K. Nikoskinen. 2001. Analysis of a three-dimensional dielectric mixture with finite difference method. *IEEE Trans. on Geoscience and Remote Sensing* 39:1013.

Kranendonk, J. van, and J. E. Sipe. 1977. Foundations of the macroscopic electromagnetic theory of dielectric media. In *Progress in Optics XV*, ed E. Wolf. New York: North-Holland.

Lamb, W., D. M. Wood, and N. W. Ashcroft. 1980. Long-wavelength electromagnetic propagation in heterogeneous media. *Phys. Rev. B* 21:2248–2266.

Lindell, I. V., A. H. Sihvola, S. A. Tretyakov, and A. J. Viitanen. 1994. *Electromagnetic waves in chiral and bi-isotropic media*. New York: Artech House.

McPhedran, R. C., and D. R. McKenzie. 1978. The conductivity of lattices of spheres: The simple cubic lattice. *Proc. R. Soc. London A* 359:45–63.

McPhedran, R. C., and D. R. McKenzie. 1978. The conductivity of lattices of spheres: The body centered and the face centered cubic lattices. *Proc. R. Soc. London A* 362:211–232.

Mittra, R., ed. 1975. *Numerical and asymptotic techniques in electromagnetics*. Topics in Applied Physics Vol. 3. Berlin: Springer-Verlag.

Moses, C. A., and N. Engheta. 2001. Electromagnetic wave propagation in the wire medium: a complex medium with long thin inclusions. *Wave Motion* 34:301–317.

Pearson, I. W. 1975. A separation of the logarithmic singularity in the exact kernel of the cylindrical antenna integral equation. *IEEE Trans. on AP* 256.

Peters, M., and E. Newman. 1995. Method of moments analysis of anisotropic artificial media composed of dielectric wire objects. *IEEE Trans. on MTT* 43:2023.

Rayleigh, ?. 1892. On the influence of obstacles arranged in rectangular order upon the properties of a medium. *Phil. Mag*. 34:481–502.

Sakoda, K. 2001. *Optical properties of photonic crystals*. Springer Series in Optical Sciences 80. Berlin: Springer-Verlag.

Sareni, B., L. Krahenbuhl, and A. Beroual. 1996. 'Effective dielectric constant of periodic composite materials. *J. Appl. Phys*. 80:1688.

Sareni, B., et al. 1997. A boundary integral equation method for the calculation of the effective permittivity of periodic composites. *IEEE Trans. on Magnetics* 33:1580.

Shivola, A. 1999. *Electromagnetic mixing formulas and applications*. IEE Electromagnetic Waves Series 47.

Silveirinha, M., and C. Fernandes. 2001. Efficient computation of the quasi-static effective permittivity of non-cubical periodic lattices. *Proc. IEEE APS/URSI Symposium*, Boston, USA, Vol. 3, 62–65.

Silveirinha, M., and C. Fernandes. 2002a. Design of a non-homogeneous wire media lens using genetic algorithms. *Proc. IEEE, APS/URSI Symposium*, San Antonio, TX, USA, Vol. 1, 730–733.

Silveirinha, M., and C. Fernandes. 2002b. Design of printed disk artificial materials. *Proc. IEEE APS/URSI Symposium*, San Antonio, TX, USA, Vol. 4, 352–355.

Silveirinha, M., and C. Fernandes. Efficient calculation of the band structure of periodic materials with cylindrical metallic inclusions. *IEEE Trans. on MTT*, in press.

Siqueira, P., and K. Sarabandi. 2000. T-matrix determination of effective permittivity for three-dimensional dense random media. *IEEE Trans. on AP* 48:317.

Whites, K. 2000. Permittivity of a multiphase and isotropic lattice of spheres at low frequency. *J. Appl. Phys*. 88:1962–1970.

Wu, F., and K. Whites. 2001. Computation of static effective permittivity for a multiphase lattice of cylinders. *Electromagnetics* 21:97.

Wu, F., and K. Whites. 2001. Quasi-static effective permittivity of periodic composites containing complex shaped dielectric particles. *IEEE Trans. on AP* 49:1174.

Yaghjian, A.. 1980. Electric dyadic Green's functions in the source region. *Proceedings IEEE* 68:248–263.